I&EC research
Industrial & Engineering Chemistry Research
pubs.acs.org/IECR
Article

SBA-15 Functionalized with Amines in the Presence of Water: Applications to CO_2 Capture and Natural Gas Desulfurization

John-Timothy Anyanwu, Yiren Wang, and Ralph T. Yang*

Cite This: *Ind. Eng. Chem. Res.* 2021, 60, 6277−6286
Read Online

ABSTRACT: Conventional and pore expanded SBA-15 were amine-grafted under dry and wet conditions using *N*[1]-(3-trimethoxysilylpropyl)diethylenetriamine. The effects of pore properties and gas hourly space velocity (GHSV) as well as the CO_2 and H_2S capture performance were investigated, and the results indicated that pore expanded SBA-15 displayed the best performance. Clumping and agglomeration of SBA-15 were observed for conventional SBA-15 under wet grafting conditions due to interparticle polymerization of amines after pores are completely filled. This phenomenon was not observed for pore expanded SBA-15, resulting in viable adsorbents with greater amounts of grafted amines. Pore expanded SBA-15 exhibited the highest CO_2 capacity (3.27 mmol/g), which to the best of our knowledge is the largest for amine-grafted adsorbents. It also exhibited high amine efficiency (0.39 mol CO_2/mol N) and faster uptake rates compared to conventional SBA-15 due to enhanced amine accessibility. For direct air capture, higher GHSV values result in lower breakthrough CO_2 capacities and the breakthrough CO_2 capacity of wet grafted pore expanded SBA-15 is more dependent on GHSV than that of dry grafted pore expanded SBA-15 due to diffusion resistance. Last, conventional SBA-15 displayed a marginally lower H_2S adsorption capacity compared to pore expanded SBA-15, suggesting that diffusion resistance does not play a significance role during H_2S adsorption. These results suggest the consideration of wet grafted pore expanded mesoporous siliceous supports for the design of promising adsorbents for the capture of CO_2 and the removal of H_2S from natural gas.

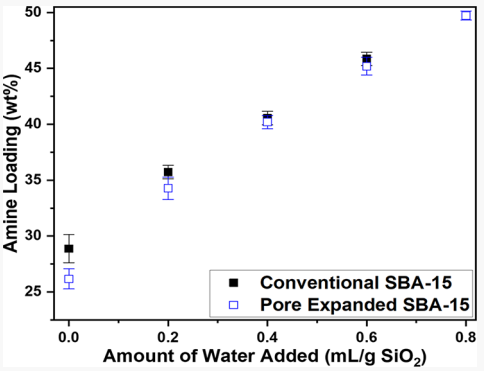

INTRODUCTION

Carbon dioxide (CO_2) is a major greenhouse gas that poses a substantial threat to the environment. The combustion of fossil fuels for energy generation has led to an unprecedented increase in CO_2 emissions.[1] Additionally, due to its corrosive and poisonous nature, hydrogen sulfide (H_2S) is another gas that needs removal during the energy generation process. Therefore, significant efforts are being undertaken to develop technologies to curb CO_2 emissions and efficiently remove H_2S.[2−8] In the past 20 years, the most promising and researched materials used for adsorption of harmful gases are zeolites, activated carbons, metal organic frameworks, and amine-functionalized mesoporous silica (silica gels, MCM-41, and SBA-15) due to their favorable porous properties.[2−35]

In particular, siliceous adsorbents functionalized with amines have been shown to be especially effective in capturing CO_2 and H_2S. Amines are used because they react with CO_2 to form carbamates under dry conditions, whereas under humid conditions, hydrogen-bonded amines are released and additional carbamate ion pairs can be formed.[28,36,37] The H_2S reaction with amines proceeds via a proton transfer mechanism, and moisture enhances the adsorption performance.[3,4] The most common methods for amine incorporation into siliceous adsorbents are through chemical grafting (covalent bonding of aminosilanes to the surface silanol groups of silica supports) and wet impregnation (impregnation of silica supports with high-molecular-weight polyamines).[2−4,10−14,16−37] While wet impregnated adsorbents attain high CO_2 capture capacity brought on by higher amine loading, they experience diffusion limitations and cyclic instability due to leaching and evaporation of the amines.[27,35,38]

In contrast, chemically grafted adsorbents are tightly tethered to the support and are less susceptible to these issues. Chemically grafted adsorbents, however, do not achieve the high capture capacity of wet impregnated adsorbents due to lower amine loadings brought on by limited availability of surface silanol groups.[39−41] In order to increase the amines loaded during the chemical grafting process, water is added during the grafting process. We hypothesize that water addition hydrates the adsorbent surface (increasing the hydroxyl groups) and also leads to the polymerization of the

Received: January 28, 2021
Revised: March 28, 2021
Accepted: April 15, 2021
Published: April 26, 2021

https://doi.org/10.1021/acs.iecr.1c00415
Ind. Eng. Chem. Res. 2021, 60, 6277−6286

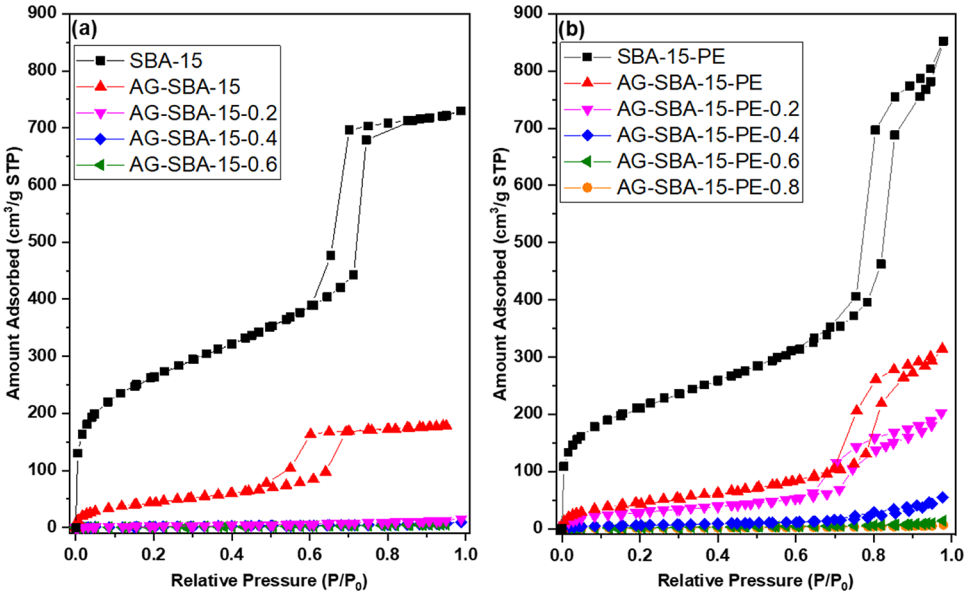

Figure 1. N_2 adsorption−desorption isotherms at −196 °C for pristine and dry and wet grafted conventional SBA-15 (a) and pore expanded SBA-15 (b).

aminosilanes via siloxane bridges of free aminosilanes to other grafted aminosilanes as proposed by Feng et al. and Harlick et al.[42,43]

At present, most of the work on wet grafting has focused on conventional SBA-15 and MCM-41 and usually at low amine loading and water addition amounts. To the best of our knowledge, there is sparse work available on the beneficial effect of utilizing pore expanded SBA-15 for wet grafting and their CO_2 adsorption performance under varied conditions.[43,44] Therefore, the objective of this study is to understand how pore structure affects amine grafting outcomes and adsorptive performance. Conventional and pore expanded SBA-15 were synthesized, and grafting (dry and wet) utilizing anhydrous N^1-(3-trimethoxysilylpropyl)diethylenetriamine ("DT") was performed. The influence of the different pore structures, amine loadings, and temperatures on the adsorbents' CO_2 capture performance was further studied. Additionally, the performance of those supports under conditions related to direct air capture, flue/post combustion gas, and natural gas sweetening was studied.

MATERIALS

N^1-(3-Trimethoxysilylpropyl)diethylenetriamine, Pluronic P123, hydrochloric acid (HCl), mesitylene, and tetraethylorthosilicate (TEOS) were obtained from Sigma Aldrich. Anhydrous toluene was obtained from Fisher Scientific.

SBA-15. The synthesis of conventional SBA-15 was performed according to the procedure reported by Wang et al.[45] Eight grams of Pluronic P123 was dissolved in 240 mL of H_2O and 40.1 mL of 37% HCl at room temperature. After the complete dissolution of Pluronic P123, the temperature was increased to 35 °C. A total of 18.2 mL of TEOS was then added to the solution dropwise. The mixture was stirred at 35 °C for 24 h followed by another 24 h at 100 °C under reflux. The resulting white solid was collected by filtration, washed with water, and dried at 50 °C overnight. Finally, it was calcined at 550 °C for 6 h under an air flow. Conventional SBA-15 was designated as SBA-15.

Pore Expanded SBA-15. The synthesis of pore expanded SBA-15 was performed according to the procedure reported by Chen et al.[46] Eight grams of Pluronic P123 was dissolved in 2.0 M aqueous HCl (320 mL) at room temperature. After the complete dissolution of Pluronic P123, the temperature was increased to 35 °C. A total of 17.8 mL of TEOS was then added to the solution dropwise and left to prehydrolyze for 30 min. After 30 min, 4.62 mL of mesitylene (1,3,5-trimethylbenzene) was added dropwise. The mixture was stirred at 35 °C for 20 h. The mixture was then autoclaved and aged for 24 h at 90 °C. The resulting white solid was collected by filtration, washed with water, and dried at 50 °C overnight. Finally, it was calcined at 550 °C for 6 h under an air flow. Pore expanded SBA-15 was designated as SBA-15-PE.

Dry Grafting. SBA-15 and SBA-15-PE were dried at 100 °C for at least 3 h prior to amine grafting. In a typical synthesis, 100 mL of anhydrous toluene was mixed with 10 mL of N^1-(3-trimethoxysilylpropyl)diethylenetriamine in an Erlenmeyer flask, and then 1 g of SBA-15 or SBA-15-PE was added. The mixture was stirred and refluxed at 85 °C for 12 h. The grafted silica was filtered, washed with copious amounts of toluene, and then dried in a 50 °C oven overnight. Dry grafted supports were designated as AG-SBA-15 and AG-SBA-15-PE.

Wet Grafting. SBA-15 and SBA-15-PE were dried at 100 °C for at least 3 h prior to amine grafting. In a typical synthesis, a specific amount of H_2O (0.2−0.8 mL) was added dropwise to a solution containing 100 mL of anhydrous toluene and 1 g of SBA-15 or SBA-15-PE. The mixture was stirred at room temperature for 2 h. A total of 10 mL of N^1-(3-trimethoxysilylpropyl)diethylenetriamine was then added. The mixture was stirred and refluxed at 85 °C for 12 h. The grafted supports were filtered, washed with copious amounts of toluene, and then dried in a 50 °C oven. Wet grafted SBA-15 was designated as AG-SBA-15-*X*, and wet grafted pore expanded SBA-15 was designated as AG-SBA-15-PE-*X*. *X* refers to the amount of water (mL H_2O/g SBA-15) added during wet grafting.

https://doi.org/10.1021/acs.iecr.1c00415
Ind. Eng. Chem. Res. 2021, 60, 6277−6286

CHARACTERIZATION

Carbon dioxide (0−1 bar) was measured on a Micromeritics ASAP 2020 Sorptometer using a volumetric technique. Carbon dioxide isotherms were measured at 25, 40 and 75, 90, and 100 °C. Nitrogen adsorption isotherms were measured at −196 °C on a Micromeritics ASAP 2020 Sorptometer. All samples were degassed overnight at 105 °C prior to all measurements. Thermogravimetric analysis was carried out on a Shimadzu TGA-50H. Amine loading analysis was performed by pretreating the sample under a helium flow for 2 h at 100 °C and then heating to 850 °C at a heating rate of 5 °C/min under a helium and air flow. Adsorption rates were examined using a TGA under a dry 70% CO_2 flow (in He) at 75 °C. Multicycle stability studies were examined using a TGA under a dry 70% CO_2 flow (in He) at 75 °C. The sample was desorbed at 90 °C in He after each adsorption cycle. Hydrogen sulfide was measured by blending predried helium with predried H_2S (200 ppm in helium). The H_2S concentration range was 0−125 ppm, and the total flow rate was 80 mL/min.

The CO_2 breakthrough adsorption measurement was performed at predetermined gas hourly space velocity (GHSV) using a vertical fixed-bed with ambient air feed in a down-flow manner. A Vaisala GMP343 CO_2 probe was used to constantly observe the CO_2 concentration of the effluent gas. The Vaisala GMP343 incorporates a silicon-based non-dispersive infrared sensor with a measurement range of 0−1000 ppm of CO_2. The fixed-bed column was 5 cm in height and 0.35 cm in diameter. The fixed-bed was held by an indent and a small piece of quartz wool. The sorbents with a particle size of 20−40 meshes were used for the breakthrough adsorption measurement. Prior to the adsorption process, the fixed-bed column was degassed at 105 °C for 3 h under nitrogen flow. Subsequently, the temperature was lowered to 25 °C and the feed gas (ambient air) was introduced at various GHSV values.

RESULTS AND DISCUSSION

Textural Properties and Amine Loading Analysis of Supports. Figure 1 shows the nitrogen adsorption−desorption isotherms at −196 °C of conventional SBA-15 and pore expanded SBA-15. The conventional supports displayed a type IV isotherm, which is indicative of a standard mesoporous material.[47,48] However, the capillary condensation step occurs at a higher relative pressure for SBA-15-PE compared to SBA-15. This proves that the addition of mesitylene (micelle expander) during synthesis led to the enlargement of the pores.[47] Furthermore, the BJH (Barrett, Joyner, and Halenda) pore size distributions are mainly centered around 8 nm for SBA-15 and 12.3 nm for SBA-15-PE. The BET surface area and total pore volume are approximately 956 m^2/g and 1.13 cm^3/g for SBA-15 and 766 m^2/g and 1.32 cm^3/g for SBA-15-PE.

Dry grafting of all supports was performed using DT, and wet grafting was accomplished using DT in the presence of water. The nitrogen adsorption−desorption isotherms at −196 °C of all amine-grafted supports are presented in Figure 1, and the pore properties are summarized in Table 1. The textural properties of conventional and pore expanded SBA-15 were provided pre- and post-grafting to convey the changes. Following dry and wet grafting, the BET surface area, pore size, and pore volume of all supports steadily decreased, confirming the presence of amine moieties in the pores. This decreasing trend is a result of blockage of pores and major coverage of the supports' surface by DT. Furthermore, this demonstrates that increasing the amine loading correlates with a decrease in surface area, pore size, and pore volume, especially after wet grafting. Thermal analysis was conducted on all dry and wet grafted adsorbents to determine the amine loadings. Weight loss before 150 °C is due to the removal of atmospheric CO_2 and adsorbed water; as such, it was omitted.[36,39−41] The decomposition of the grafted amine occurs above 150 °C and leveled off around 600 °C. As shown in Figure 2, the amine loadings of dry grafted conventional and pore expanded SBA-15 were 26 and 28%, respectively. This disparity corresponds to the BET surface area of their respective pristine supports. Post-wet grafting, the amine loading increased from 28 to 46% for conventional SBA-15 and 26 to 50% for pore expanded SBA-15. This suggests conclusively that the addition of water during the grafting process successfully led to the increased amine loading. Despite the initial difference in amine loading for dry grafted AG-SBA-15 and AG-SBA-15-PE, however, the amine loading after wet grafting is similar when 0.2−0.6 mL H_2O/g SBA-15 is added. This indicates that higher BET surface area, pore size, and pore volume are not correlated with higher amine loading for wet grafted adsorbents. It also suggests that silanol density,

Table 1. Surface Area and Pore Structure Parameters

sample	BET surface area (m^2/g)	pore diameter (nm)	total pore volume (cm^3/g)
SBA-15	956	7.87	1.13
AG-SBA-15	168	6.39	0.276
AG-SBA-15-0.2	12.7	5.65	0.0236
AG-SBA-15-0.4	9.25	4.28	0.0104
AG-SBA-15-0.6	9.7	3.1	0.00823
SBA-15-PE	766	12.3	1.32
AG-SBA-15-PE	177	10.7	0.0486
AG-SBA-15-PE-0.2	112	7.87	0.0314
AG-SBA-15-PE-0.4	25.5	10	0.00856
AG-SBA-15-PE-0.6	9.64	4.67	0.00216
AG-SBA-15-PE-0.8	5.04	3.63	0.00104

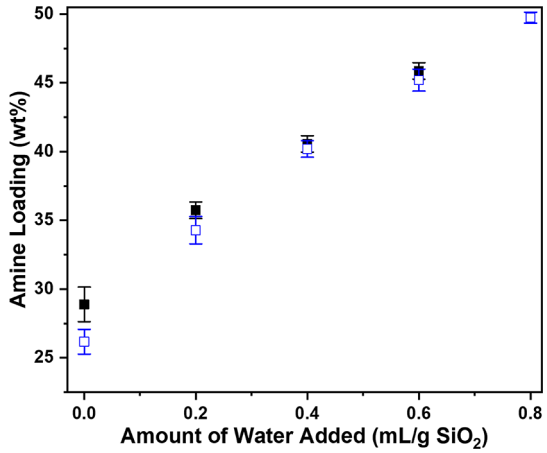

Figure 2. Amine loading of conventional SBA-15 (closed symbol) and pore expanded SBA-15 (open symbols) using different amounts of water during grafting.

https://doi.org/10.1021/acs.iecr.1c00415
Ind. Eng. Chem. Res. 2021, 60, 6277−6286

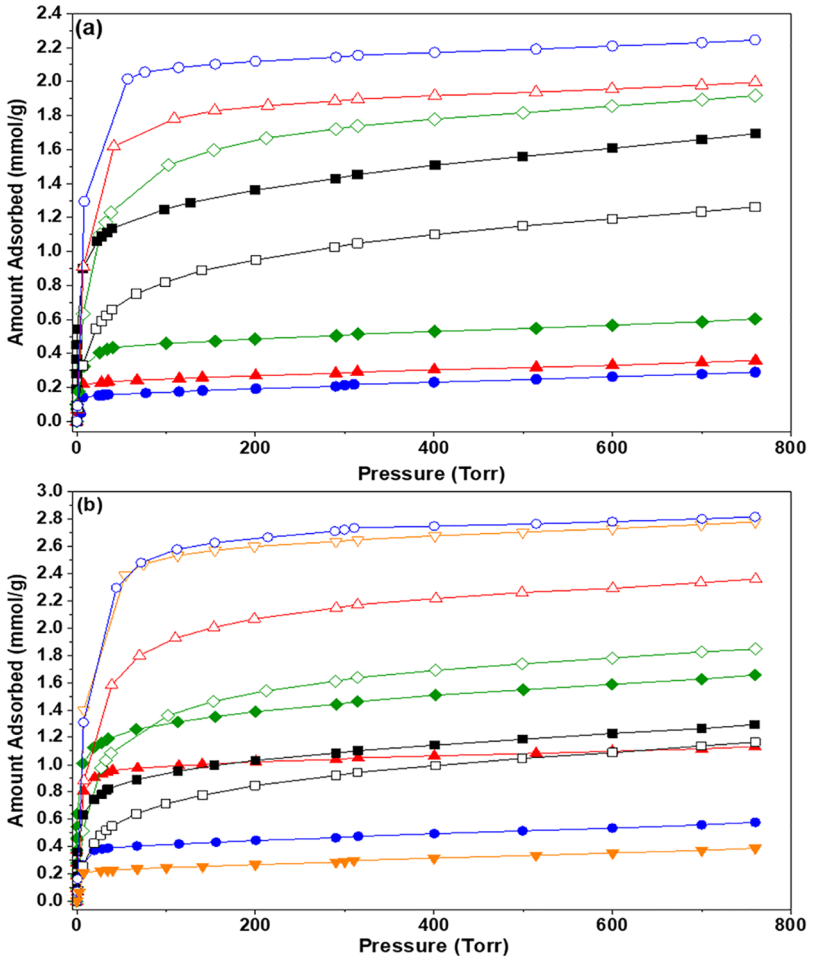

Figure 3. CO_2 adsorption isotherms at 25 °C (closed symbols) and 75 °C (open symbols) for conventional SBA-15 (a) and pore expanded SBA-15 (b) using 0 mL of H_2O (squares), 0.2 mL of H_2O (diamonds), 0.4 mL of H_2O (triangles), 0.6 mL of H_2O (circles), and 0.8 mL of H_2O (inverted triangles).

typically correlated with amine loading of dry grafting adsorbents, does not affect the amine loading of wet grafted adsorbents. Nonetheless, further investigation is needed to reach a conclusion.

Under the reported synthesis conditions, the continuous addition of water (0.2−0.8 mL H_2O/g SBA-15) increased the amine loading of conventional and pore expanded SBA-15 without signs of plateauing. Notably, addition beyond 0.6 mL of water resulted in the clumping and agglomeration of conventional SBA-15. This is possibly due to interparticle polymerization of amines after the pores are completely filled. The agglomeration of SBA-15 was not observed for pore expanded SBA-15 beyond addition of 0.6 mL of water. This is likely because of the larger pore size of SBA-15-PE, allowing for greater amounts of grafted amines. This is supported by the nitrogen adsorption−desorption results summarized in Table 1. Following wet grafting with 0.6 mL H_2O/g SBA-15, SBA-15-PE maintained more of their porosity (4.67 nm) compared to SBA-15 (3.1 nm), indicating the importance of larger pore sizes for continuously increasing water addition during grafting to attain higher amine loadings.

CO_2 Capture Performance. *Effects of Amine Loading and Temperature on CO_2 Adsorption.* The CO_2 adsorption performance of dry grafted and wet grafted supports at 25 and 75 °C at different amine loadings is compared in Figure 2. The CO_2 adsorption capacities at 25 and 75 °C and 1 bar are 1.69 and 1.26 mmol/g for AG-SBA-15 and 1.29 and 1.16 mmol/g for AG-SBA-15-PE. Upon wet grafting, the CO_2 adsorption capacities at 25 °C and 1 bar are 0.60 mmol/g (AG-SBA-15-0.2), 0.35 mmol/g (AG-SBA-15-0.4), and 0.29 mmol/g (AG-SBA-15-0.6).

The CO_2 adsorption capacities at 25 °C for wet grafted pore expanded SBA-15 are 1.66 mmol/g (AG-SBA-15-PE-0.2), 1.13 mmol/g (AG-SBA-15-PE-0.4), 0.58 mmol/g (AG-SBA-15-PE-0.6), and 0.39 mmol/g (AG-SBA-15-PE-0.8). The adsorption capacities at 75 °C and 1 bar are 1.92 mmol/g (AG-SBA-15-0.2), 2 mmol/g (AG-SBA-15-0.4), and 2.24 mmol/g (AG-SBA-15-0.6). For wet grafted pore expanded SBA-15, the adsorption capacities are 1.85 mmol/g (AG-SBA-15-PE-0.2), 2.36 mmol/g (AG-SBA-15-PE-0.4), 2.82 mmol/g (AG-SBA-15-PE-0.6), and 2.78 mmol/g (AG-SBA-15-PE-0.8). Significantly, for AG-SBA-15-0.2, the adsorption capacity decreased at 25 °C. Conversely, the adsorption capacity increased for AG-SBA-15-PE-0.2 before decreasing upon a further increase in amine concentration. For CO_2 adsorption at 25 °C, there is an initial enhancement of the CO_2 capture capacity for wet grafted adsorbents at their optimal water addition amounts. In this instance, the optimal amount is 0.2 mL H_2O/g SBA-15 for SBA-15-PE and a further increase in the water addition amount during grafting results in a decrease in the adsorption capacity at 25 °C. This suggests that the optimal water addition amount for high CO_2 adsorption capacity at 25 °C is dependent on the

https://doi.org/10.1021/acs.iecr.1c00415
Ind. Eng. Chem. Res. 2021, 60, 6277−6286

Table 2. Summary of Wet Grafted Silica Adsorbents and Their CO_2 Capture Capacities

		CO_2 adsorption capacity			
sample	amine used	CO_2 partial pressure (bar)	temperature (°C)	adsorption capacity (mmol/g, dry)	reference
silica gel	triamine	1	75	2.3	32
MCM-41	triamine	0.2	75	2.1	60
KIT-6	APTES	1	75	1.31	61
SBA-15	diamine	0.15	60	1.36	62
SBA-15	triamine	0.15	60	1.58	62
SBA-15	triamine	0.89	75	2.3	63
AG-SBA-15-PE-0.6	triamine	0.15	75	2.58	present work
AG-SBA-15-PE-0.6	triamine	1	75	2.82	present work
AG-SBA-15-PE-0.6	triamine	1	90	3.03	present work

support's pore structure. Additionally, the adsorption capacity at 25 °C for conventional SBA-15 reduced as the amine loading increased. The increase in amine loading for silica adsorbents is due to the hydrolysis and condensation of alkoxy groups in the presence of water, leading to aminosilane polymerization. The degree of polymerization is dictated by the amount of water added to the solution for alkoxy hydrolysis and condensation. The polymerization of amines at high water addition amounts clogs the pores, which results in reduced adsorption capacity at 25 °C.[49,50]

Moreover, the adsorption capacity at 75 °C for all supports rose substantially as the amine loading increased. This marked increase is attributable to the decreased viscosity and increased mobility of the polymer-like amines at 75 °C, leading to the accessibility of more amine sites for CO_2 molecules.[17,36,51,52] The higher adsorption capacity of amine-grafted pore expanded SBA-15 compared to conventional SBA-15 is due to the large pore size of the pore expanded supports. Supports with large pores provide increased accessibility of the densely grafted amines; however, there is a point at which the increase in amine concentration ceases to increase the CO_2 uptake of large pore supports. When the water addition amount is increased to 0.8 mL H_2O/g SBA-15, the amine loading increases to 50%. The CO_2 adsorption capacity, however, decreases from 2.81 mmol/g (AG-SBA-15-PE-0.6) to 2.78 mmol/g (AG-SBA-15-PE-0.8) at 75 °C. The pore channels of AG-SBA-15-PE-0.8 were clogged by the large amounts of grafted amines, thus hindering the adsorption of CO_2. This underscores the importance of determining the optimal water addition amount to attain the best adsorption performance.

Adsorbent performance under conditions related to flue/post combustion is important. Flue gas needs to be cooled to around 44−100 °C, and as such, understanding the adsorbent's performance in that temperature range is the key. Investigating the effect of adsorption temperature on wet grafted adsorbents with different pore properties is also essential. Consequently, CO_2 adsorption isotherms for all supports (Figure 3 and Figures S1 and S2 in the Supporting Information) were plotted to address those concerns. Regardless of the pore structure of the SBA-15 supports, the CO_2 adsorption capacity of all dry grafted adsorbents achieved their highest CO_2 capacity at 25 °C followed by 75 °C. This observed decrease in CO_2 adsorption capacity after the adsorption temperature is increased demonstrates the exothermic nature of CO_2 adsorption. Furthermore, the CO_2 adsorption capacity for all wet grafted supports increased significantly as the adsorption temperature was increased from 25 to 75 °C. However, as shown in Table S1, the trends beyond 75 °C are not as clear-cut. The CO_2 adsorption capacities of conventional and pore expanded supports grafted in greater than 0.4 mL H_2O/g SBA-15 were highest at 90 °C; however, at 100 °C, the adsorption capacity began to decrease. One of the main adsorption barriers for supports with large amounts of grafted amines is the diffusion of CO_2 on the surface to the bulk of the grafted amines. The increase in temperature to 90 °C renders the amines more mobile and facilitates the transfer of adsorbed CO_2 from the surface into the bulk of the amines, thereby revealing more amine sites for CO_2 adsorption and greatly improving the CO_2 adsorption capacity. Conversely, while higher temperatures reveal more amine sites, the desorption of CO_2 from amine sites is more preferential, resulting in the reduced adsorption capacity at 100 °C.[17,36,51−53] It is worth noting that for AG-SBA-15-PE-0.6, the best performing adsorbent, the CO_2 adsorption capacity increased from 0.42 mmol/g (25 °C) to 2.58 mmol/g (75 °C) in the flue gas range (∼0.15 bar), as shown in Figure S3. Increasing the adsorption temperature beyond 75 °C resulted in a decrease in the adsorption capacity in the flue gas range. Namely, at 90 and 100 °C (∼0.15 bar), the CO_2 adsorption capacity decreased to 2.2 and 1.7 mmol/g, respectively. The CO_2 adsorption capacity at 1 bar increased from 0.58 mmol/g (25 °C) to 3.03 mmol/g (90 °C) before decreasing to 2.86 mmol/g at 100 °C. It is likely that the aforementioned adsorption barriers also manifest in the flue gas range.

Amine efficiency (mol CO_2/mol N) is an additional component to examine for amine-grafted supports. Under dry conditions, the maximum theoretical amine efficiency is 0.5 mol CO_2/mol N. Values above 0.5 can be achieved in the presence of moisture.[28,29,36] Several factors including steric hindrances from surrounding amine groups, pore clogging or blockage, and amine location inside pores play a role in decreasing amine efficiency. The maximum amine efficiencies of all grafted supports at 25, 75, 90, and 100 °C are summarized in Table S1. At 25 °C, the amine efficiency of AG-SBA-15-*X* and AG-SBA-15-PE-*X* decreases gradually as the water addition amount and the amine loading increase. However, at 75, 90, and 100 °C, the amine efficiency trends are not as unambiguous. There is an initial increase in the amine efficiency of AG-SBA-15 from 0.25 to 0.31 for AG-SBA-15-0.2 at higher adsorption temperatures; however, as the amine loading increases, the amine efficiency stays relatively flat thereafter. The amine efficiency trends are similar for pore expanded SBA-15 at 75, 90, and 100 °C. The amine efficiency increases from 0.26 for AG-SBA-15-PE to 0.32 for AG-SBA-15-PE-0.2. At higher amounts of water addition (0.4−0.6 mL H_2O/g SBA-15) and higher adsorption temperatures (75−100 °C), the amine efficiency continues to increase before declining slightly for AG-SBA-15-PE-0.8. Generally, the

https://doi.org/10.1021/acs.iecr.1c00415
Ind. Eng. Chem. Res. 2021, 60, 6277−6286

amine efficiency for wet grafted pore expanded SBA-15 when compared to all wet grafted conventional SBA-15 is noticeably higher. Although wet grafted conventional and pore expanded SBA-15 displayed very similar amine loadings, they achieved significantly different adsorption capacities and amine efficiencies. The large pore size (12.3 nm vs 8 nm) of SBA-15-PE compared to SBA-15 reduces mass transfer resistance, leading to enhanced adsorption performance. This demonstrates that supports with favorable physical characteristics (large pore size) alleviate accessibility concerns emerging from large amine loadings, leading to higher amine utilization.

To date, research on wet grafted adsorbents mainly utilizes conventional supports. Table 2 outlines the results from this work and the literature utilizing similar methods. The increased wet grafted pore expanded SBA-15 is highly competitive, with similar or higher CO_2 adsorption capacity than all reported adsorbents.

Uptake Rates. The adsorption rates of CO_2 were measured for conventional and pore expanded SBA-15 at 75 °C using the gravimetric method. The measurement was carried out by introducing the amine-grafted adsorbents to a 70% CO_2/He feed gas mixture at time = 0, from an initial helium flow, at the desired temperature. The thermogravimetric data was used to calculate the diffusion time constant. The diffusion time constant (D/R^2, where D is the pore diffusivity and R is the radius of the particle) is used to express the uptake rates.[36,39,54,55] The calculated D/R^2 values are outlined in Table 3. As listed in Table 3, the uptake rates for wet grafted SBA-15-PE are significantly higher than those of wet grafted SBA-15. More precisely, the D/R^2 of AG-SBA-15-PE-0.6 is 23 times that of AG-SBA-15-0.6 at 75 °C. Higher uptake rates for AG-SBA-15-PE-0.6 are due to its favorable pore structure, leading to increased accessibility of the amine groups. Despite similar amine loadings for AG-SBA-15-0.6 and AG-SBA-15-PE-0.6, AG-SBA-15-PE-0.6 exhibits higher uptake rates than AG-SBA-15-0.6. This indicates that there are marked diffusion limitations for smaller pore supports with high amine loadings. These limitations are diminished for larger pore supports because they allow the CO_2 molecules easier access to available amine groups.

Table 3. Diffusion Time Constants (D/R^2) for Dry and Wet Grafted Conventional and Pore Expanded SBA-15 at 75 °C

sample	D/R^2 (1×10^{-5}) (s^{-1})
AG-SBA-15	110
AG-SBA-15-0.2	7.1
AG-SBA-15-0.4	4.9
AG-SBA-15-0.6	3.6
AG-SBA-15-PE	127
AG-SBA-15-PE-0.2	95
AG-SBA-15-PE-0.4	90
AG-SBA-15-PE-0.6	84
AG-SBA-15-PE-0.8	13

Cyclic Stability. It is crucial that adsorbents be stable after multiple adsorption/desorption cycles if they are to be applied practically. The multicycle stability of AG-SBA-15-PE-0.6 (highest performing support) was carried out at 75 °C. AG-SBA-15-PE-0.6 was regenerated at 90 °C in He after each adsorption measurement, and it took roughly 2 min to regenerate fully. There was no significant loss in CO_2 adsorption capacity at 75 °C (Figure 4) after 11 cycles. The

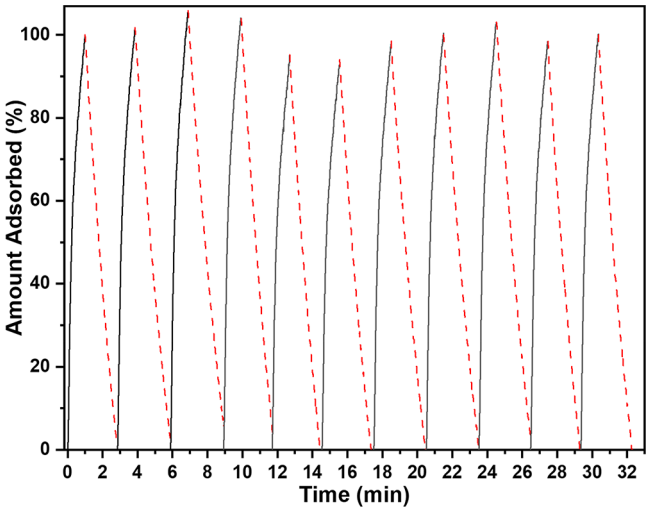

Figure 4. Cyclic stability studies (70% CO_2 (in He) flow; desorption in He at 90 °C (dashed line)) of wet grafted AG-SBA-15-PE at 75 °C and 1 bar.

CO_2 adsorption capacity did not change significantly after numerous adsorption/desorption cycles, which is consistent with the previous findings for wet grafted adsorbents and indicates that AG-SBA-15-PE-0.6 displays stability over multiple cycles.[16,31,36,38] Under dry conditions, however, the stability of the adsorbent will eventually deteriorate.[31,38] This deterioration largely results from the formation of stable urea groups after continued cycling of the adsorbent at high temperatures. Carbamate decomposition might also play a role in the deterioration. Stable urea groups deactivate grafted amine, but, provided that CO_2 adsorption is performed under wet conditions, the formation of urea groups is strongly inhibited.[56] Sayari and Belmabkhout measured the adsorption capacity of amine-grafted MCM-41 under wet conditions (0.4% R.H., 70 °C) for 700 cycles, and there was no observable loss.[56] This phenomenon is likely to be exhibited in other amine-functionalized silica, namely, AG-SBA-15-PE-0.6.

Effect of Gas Hourly Space Velocity. The effect of the GHSV on the adsorption performance of AG-SBA-15-PE and AG-SBA-15-PE-0.6 and the dependence of the breakthrough CO_2 capacity on the space velocity were examined at 25 °C, 400 ppm CO_2, and GHSV values ranging from 2000 to 20,000 h^{-1} for direct air capture applications. The breakthrough results are displayed in Figures 5 and 6 and Table 4. At GHSV values of 2000, 4000, and 20,000 h^{-1}, the measured breakthrough CO_2 capacities were 0.422, 0.279, and 0.177 mmol/g for dry grafted AG-SBA-15-PE and 0.149, 0.112, and 0.040 mmol/g for wet grafted AG-SBA-15-PE-0.6. As the GHSV was increased from 2000 to 20,000, the breakthrough CO_2 capacities decreased by approximately 58 and 73% for dry grafted AG-SBA-15-PE and wet grafted AG-SBA-15-PE-0.6, respectively. Higher GHSV values clearly result in lower breakthrough CO_2 capacities, and the breakthrough CO_2 capacity of wet grafted SBA-15-PE is evidently more dependent on GHSV than dry grafted SBA-15-PE due to diffusion resistance. Moreover, at the same GHSV values, the breakthrough curves of dry grafted AG-SBA-15-PE are much steeper than those of wet grafted AG-SBA-15-PE-0.6, further confirming the higher D/R^2 of dry grafted AG-SBA-15-PE.[57]

H_2S Adsorption Performance. Another harmful gas that needs to be removed from natural gas is hydrogen sulfide

https://doi.org/10.1021/acs.iecr.1c00415
Ind. Eng. Chem. Res. 2021, 60, 6277−6286

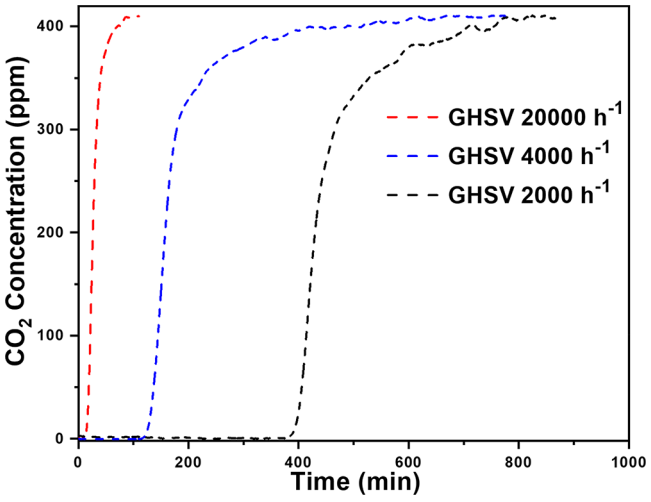

Figure 5. CO_2 breakthrough curves for AG-SBA-15-PE under an ambient air feed at 25 °C, 0.96 bar, and different GHSV values.

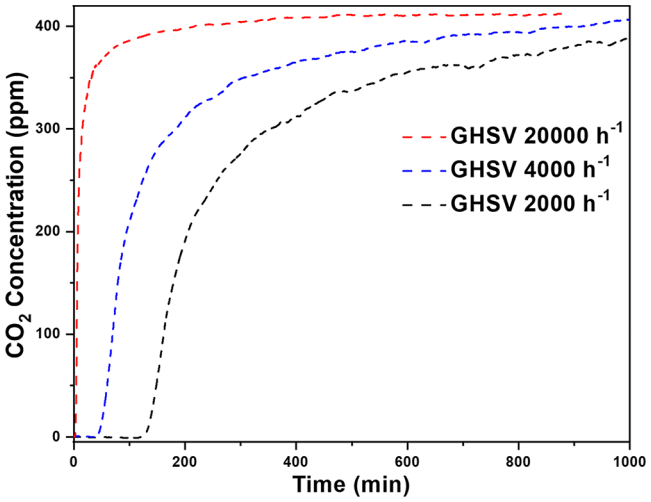

Figure 6. CO_2 breakthrough curves for AG-SBA-15-PE-0.6 under an ambient air feed at 25 °C, 0.96 bar, and different GHSV values.

Table 4. CO_2 Breakthrough Capacity for Amine-Grafted SBA-15-PE under an Ambient Air Feed at 25 °C, 0.96 bar, 0.0% R.H., and Different GHSV Values

	GHSV (h^{-1})		
sample	2000	4000	20,000
AG-SBA-15-PE	0.422 mmol/g	0.279 mmol/g	0.177 mmol/g
AG-SBA-15-PE-0.6	0.149 mmol/g	0.112 mmol/g	0.040 mmol/g

(H_2S). The low-concentration H_2S adsorption isotherms at 25 and 50 °C of AG-SBA-15-PE and AG-SBA-15-PE-0.6 are presented in Figure 7. The results suggest that H_2S adsorption is favorable for supports with high amine loadings. Additionally, it is notable that even at higher amine loading, H_2S adsorption was not influenced by adsorption temperature in the same way that CO_2 was. The maximum CO_2 adsorption capacity of all wet grafted adsorbents increased from 25 to 90 °C, whereas for H_2S, the adsorption capacity decreased from 25 to 50 °C for AG-SBA-15-0.6 and AG-SBA-15-PE-0.6. A further increase in the adsorption temperature beyond 50 °C led to negligible H_2S adsorption. Ma et al. observed a similar behavior for PEI-impregnated MCM-41 and attributed this to

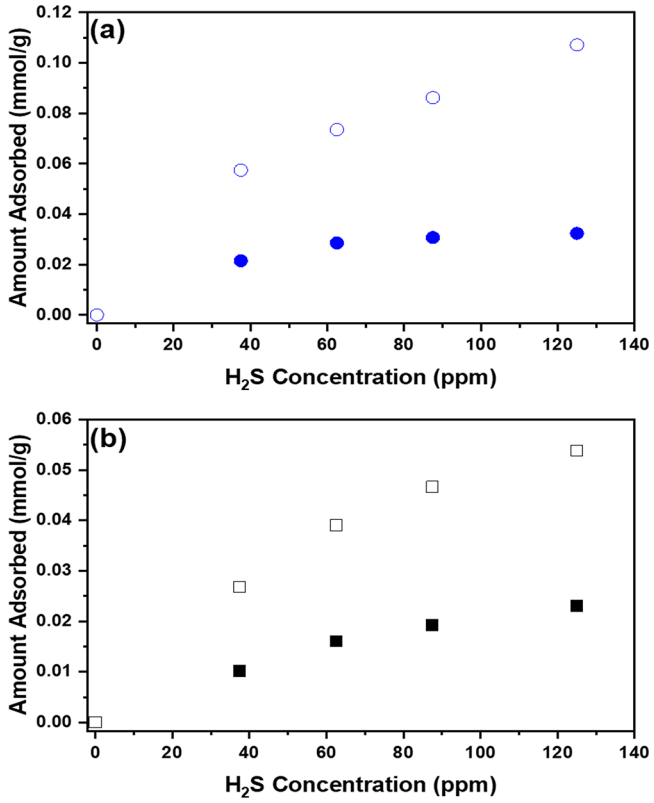

Figure 7. H_2S adsorption isotherms for AG-SBA-15-PE-0.6 (a) and AG-SBA-15-PE (b) at 25 °C (open symbols) and 50 °C (closed symbols) and 1 bar.

significantly lower diffusion limitations for H_2S.[7] They reported that the estimated kinetic barrier for diffusion of H_2S from the adsorbent surface into the bulk of the amine is approximately three times lower than that of CO_2, suggesting that H_2S is predominantly thermodynamically controlled since lower temperatures thermodynamically favor CO_2 and H_2S adsorption. To further expand on their work, the H_2S adsorption capacities of AG-SBA-15-0.6 and AG-SBA-15-PE-0.6 were compared in Figure 8 to determine if large pore supports provide any enhancement in adsorption performance.

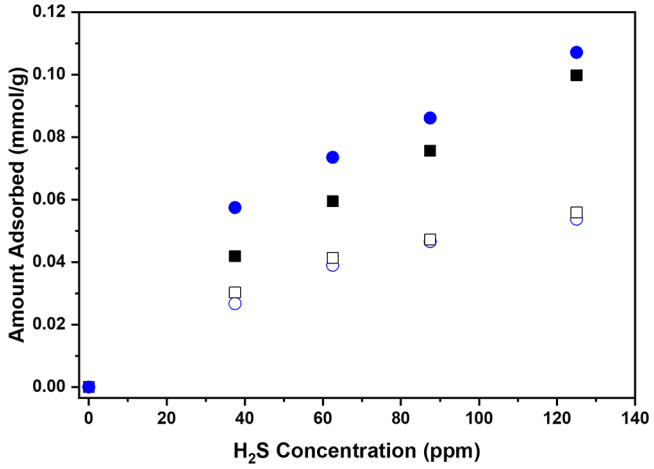

Figure 8. H_2S adsorption isotherms for AG-SBA-15 (open squares), AG-SBA-15-PE (open circles), AG-SBA-15-0.6 (closed squares), and AG-SBA-15-PE-0.6 (closed circles) at 25 °C and 1 bar.

https://doi.org/10.1021/acs.iecr.1c00415
Ind. Eng. Chem. Res. 2021, 60, 6277−6286

Despite similar amine loadings, AG-SBA-15-PE-0.6 exhibited a marginally higher H_2S adsorption capacity at 25 °C than AG-SBA-15-0.6. The H_2S adsorption capacities at 25 °C are 0.11 mmol/g (AG-SBA-15-PE-0.6) and 0.099 mmol/g (AG-SBA-15-0.6). Unlike CO_2 that displayed a 100% increase in the adsorption capacity at 25 °C for pore expanded SBA-15 (Table S1), large pore supports do not significantly enhance H_2S adsorption capacity. This is further elucidated by the amine efficiency (mol H_2S/mol N). AG-SBA-15-PE-0.6 displayed a marginally higher amine efficiency (0.014) compared to AG-SBA-15-0.6 (0.012).

Overall, despite the high amine loadings, the H_2S adsorption capacities reduced as the adsorption temperature was increased, indicating that the adsorption process of H_2S was thermodynamically controlled. Conventional SBA-15 displayed a slightly lower H_2S adsorption capacity compared to pore expanded SBA-15 (Figure 8), confirming that diffusion resistance does not play a significance role during H_2S adsorption.

While AG-SBA-15-PE-0.6 does not exhibit the high H_2S capacities of zeolites, it does not suffer from diminished adsorption performance under wet conditions.[58,59] In fact, Okonkwo et al. found that for amine-grafted adsorbents, moisture has a positive effect on the H_2S adsorption capacity.[3] They reported higher H_2S adsorption capacity and good H_2S selectivity in the presence of CO_2 for amine-grafted SBA-15 adsorbents. For zeolites, however, there is an observed negative influence due to competition for amine sites.

The pure component methane isotherm of AG-SBA-15-PE and AG-SBA-15-PE-0.6 at 25 °C is presented in Figure 9. The

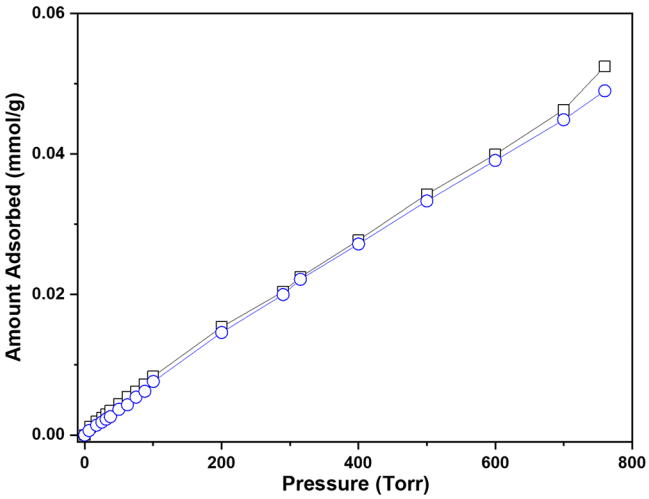

Figure 9. CH_4 adsorption isotherm for AG-SBA-15-PE (open squares) and AG-SBA-15-PE-0.6 (open circles) at 25 °C and 1 bar.

H_2S adsorption capacities at 25 and 50 °C are 0.054 and 0.023 mmol/g for AG-SBA-15-PE and 0.11 and 0.032 mmol/g for AG-SBA-15-PE-0.6, respectively. The methane adsorption capacity is 0.04 mmol/g at 25 °C and 760 torr. The methane adsorption capacity is substantially lower at 760 torr compared to the H_2S adsorption at a much lower concentration (125 ppm). This indicates that the increased amine concentration resulted in a minimal increase in the methane capacity. However, the H_2S adsorption capacity increased by 99% with the increase in amine loading. These properties make AG-SBA-15-PE-0.6 a suitable adsorbent for natural gas desulfurization.

CONCLUSIONS

In this work, conventional and pore expanded SBA-15 were amine-grafted (dry and wet) using DT. The results indicate that amine-grafted pore expanded SBA-15 with large pore size and pore volume has a positive effect on carbon dioxide adsorption performance. The large pore size reduces mass transfer resistance, leading to enhanced adsorption performance. Wet grafted pore expanded SBA-15 resulted in CO_2 adsorption capacities of 2.8 mmol/g at 75 °C and ∼0.15 bar and 2.99 mmol/g at 75 °C and 1 bar. The CO_2 adsorption capacity increased to 3.30 mmol/g at 90 °C and 1 bar. To the best of our knowledge, these are the highest reported CO_2 adsorption capacity for DT-grafted adsorbents and the first experimental evidence for the positive effect of high temperatures (>75 °C) on amine-grafted SBA-15. Moreover, pore expanded SBA-15 displayed enhanced amine efficiencies, and CO_2 uptake rates compared to conventional SBA-15. AG-SBA-15-PE-0.6 showed stability over 10 adsorption/desorption cycles. The H_2S adsorption performance indicates that AG-SBA-15-PE-0.6 is a viable adsorbent for the sweetening of methane-containing gases. These excellent CO_2 and H_2S capture characteristics indicate that wet grafted pore expanded SBA-15 can be considered a promising amine-functionalized adsorbent for flue gas CO_2 and H_2S capture applications.

ASSOCIATED CONTENT

Supporting Information

The Supporting Information is available free of charge at https://pubs.acs.org/doi/10.1021/acs.iecr.1c00415.

Table of CO_2 adsorption capacity, amine loading, and amine efficiency of all adsorbents; CO_2 adsorption isotherms at 90 and 100 °C for conventional and pore expanded SBA-15; CO_2 adsorption capacities at ∼0.15 bar for wet grafted conventional and pore expanded SBA-15 at 25 and 75 °C; and TGA thermograms of dry and wet grafted conventional and pore expanded SBA-15 (PDF)

AUTHOR INFORMATION

Corresponding Author

Ralph T. Yang − *Department of Chemical Engineering, University of Michigan, Ann Arbor, Michigan 48109, United States;* orcid.org/0000-0002-5367-9550; Email: yang@umich.edu

Authors

John-Timothy Anyanwu − *Department of Chemical Engineering, University of Michigan, Ann Arbor, Michigan 48109, United States*

Yiren Wang − *Department of Chemical Engineering, University of Michigan, Ann Arbor, Michigan 48109, United States*

Complete contact information is available at: https://pubs.acs.org/10.1021/acs.iecr.1c00415

Notes

The authors declare no competing financial interest.

ACKNOWLEDGMENTS

This work was supported by NSF Grant CBET-1826621, the Global CO_2 Initiative at the University of Michigan and the

Blue Sky program of the College of Engineering at the University of Michigan.

REFERENCES

(1) Vitillo, J. G.; Smit, B.; Gagliardi, L. Introduction: Carbon Capture and Separation. *Chem. Rev.* **2017**, *117*, 9521−9523.
(2) Okonkwo, C. N.; Okolie, C.; Sujan, A.; Zhu, G.; Jones, C. W. Role of Amine Structure on Hydrogen Sulfide Capture from Dilute Gas Streams Using Solid Adsorbents. *Energy Fuels* **2018**, *32*, 6926−6933.
(3) Okonkwo, C. N.; Fang, H.; Sholl, D. S.; Leisen, J. E.; Jones, C. W. Effect of Humidity on the Sorption of H2S from Multicomponent Acid Gas Streams on Silica-Supported Sterically Hindered and Unhindered Amines. *ACS Sustainable Chem. Eng.* **2020**, *8*, 10102−10114.
(4) Okonkwo, C. N.; Lee, J. J.; De Vylder, A.; Chiang, Y.; Thybaut, J. W.; Jones, C. W. Selective Removal of Hydrogen Sulfide from Simulated Biogas Streams Using Sterically Hindered Amine Adsorbents. *Chem. Eng. J.* **2020**, *379*, 122349.
(5) Huang, H. Y.; Yang, R. T.; Chinn, D.; Munson, C. L. Amine-Grafted MCM-48 and Silica Xerogel as Superior Sorbents for Acidic Gas Removal from Natural Gas. *Ind. Eng. Chem. Res.* **2003**, *42*, 2427−2433.
(6) Belmabkhout, Y.; De Weireld, G.; Sayari, A. Amine-Bearing Mesoporous Silica for CO_2 and H_2S Removal from Natural Gas and Biogas. *Langmuir* **2009**, *25*, 13275−13278.
(7) Ma, X.; Wang, X.; Song, C. "Molecular Basket" Sorbents for Separation of CO_2 and H_2S from Various Gas Streams. *J. Am. Chem. Soc.* **2009**, *131*, 5777−5783.
(8) Belmabkhout, Y.; Heymans, N.; De Weireld, G.; Sayari, A. Simultaneous Adsorption of H_2S and CO_2 on Triamine-Grafted Pore-Expanded Mesoporous MCM-41 Silica. *Energy Fuels* **2011**, *25*, 1310−1315.
(9) Moran, C. M.; Marti, R. M.; Joshi, J. N.; Hayes, S. E.; Walton, K. S. Tuning Residual Metal in Partially Etched Carbide-Derived Carbons for Enhanced Acid Gas Adsorption. *Carbon N. Y.* **2020**, *158*, 481−493.
(10) Lyndon, R.; You, W.; Ma, Y.; Bacsa, J.; Gong, Y.; Stangland, E. E.; Walton, K. S.; Sholl, D. S.; Lively, R. P. Tuning the Structures of Metal−Organic Frameworks via a Mixed-Linker Strategy for Ethylene/Ethane Kinetic Separation. *Chem. Mater.* **2020**, *32*, 3715−3722.
(11) Huang, Y.; Jiao, Y.; Chen, T.; Gong, Y.; Wang, S.; Liu, Y.; Sholl, D. S.; Walton, K. S. Tuning the Wettability of Metal-Organic Frameworks via Defect Engineering for Efficient Oil/Water Separation. *ACS Appl. Mater. Interfaces* **2020**, *12*, 34413−34422.
(12) Walton, I.; Chen, C.; Rimsza, J. M.; Nenoff, T. M.; Walton, K. S. Enhanced Sulfur Dioxide Adsorption in UiO-66 through Crystal Engineering and Chalcogen Bonding. *Cryst. Growth Des.* **2020**, *20*, 6139−6146.
(13) Batra, R.; Chen, C.; Evans, T. G.; Walton, K. S.; Ramprasad, R. Prediction of Water Stability of Metal−Organic Frameworks Using Machine Learning. *Nat. Mach. Intell.* **2020**, *2*, 704−710.
(14) Burtch, N. C.; Walton, I. M.; Hungerford, J. T.; Morelock, C. R.; Jiao, Y.; Heinen, J.; Chen, Y. S.; Yakovenko, A. A.; Xu, W.; Dubbeldam, D.; et al. In Situ Visualization of Loading-Dependent Water Effects in a Stable Metal−Organic Framework. *Nat. Chem.* **2020**, *12*, 186−192.
(15) de Oliveira, J. L. B.; Nascimento, B. O.; Gonçalves, D. V.; Santiago, R. G.; de Lucena, S. M. P.; de Azevedo, D. C. S.; Bastos-Neto, M. Effect of Ultramicropores on the Mechanisms of H2S Retention from Biogas. *Chem. Eng. Res. Des.* **2020**, *154*, 241−249.
(16) Santiago, R. G.; Siqueira, R. M.; Alves, C. A.; Vilarrasa-García, E.; Maia, D. A. S.; Bastos-Neto, M.; de Azevedo, D. C. S. Evaluation of the Thermal Regeneration of an Amine-Grafted Mesoporous Silica Used for CO2/N2 Separation. *Adsorption* **2020**, *26*, 203−215.
(17) Sánchez-Zambrano, K. S.; Vilarrasa-García, E.; Maia, D. A. S.; Bastos-Neto, M.; Rodríguez-Castellon, E.; Azevedo, D. C. S. Adsorption Microcalorimetry as a Tool in the Characterization of Amine-Grafted Mesoporous Silicas for CO2 Capture. *Adsorption* **2020**, *26*, 165−175.
(18) Silva, E. N.; Cantillo-Castrillon, M.; Dantas, T. M.; Mesquita, Y. M.; Maia, D. A. S.; Bastos-Neto, M.; Barcellos, W. M.; Azevedo, D. C. S. Siloxane Adsorption by Porous Silica Synthesized from Residual Sand of Wastewater Treatment. *J. Environ. Chem. Eng.* **2020**, 104805.
(19) Liu, Y.; Liu, J.; Lin, Y. S. Strong Binding Site Molarity of MOFs and Its Effect on CO2 Adsorption. *Microporous Mesoporous Mater.* **2015**, *214*, 242−245.
(20) Liu, Y.; Hu, J.; Ma, X.; Liu, J.; Lin, Y. S. Mechanism of CO2 Adsorption on Mg/DOBDC with Elevated CO2 Loading. *Fuel* **2016**, *181*, 340−346.
(21) Rui, Z.; James, J. B.; Kasik, A.; Lin, Y. S. Metal-Organic Framework Membrane Process for High Purity CO_2 Production. *AIChE J.* **2016**, *62*, 3836−3841.
(22) Rui, Z.; James, J. B.; Lin, Y. S. Highly CO2 Perm-Selective Metal-Organic Framework Membranes through CO2 Annealing Post-Treatment. *J. Memb. Sci.* **2018**, *555*, 97−104.
(23) Wilson, S. M. W.; Tezel, F. H. Direct Dry Air Capture of CO_2Using VTSA with Faujasite Zeolites. *Ind. Eng. Chem. Res.* **2020**, *59*, 8783−8794.
(24) Wilson, S. M. W.; Kennedy, D. A.; Tezel, F. H. Adsorbent Screening for CO2/CO Separation for Applications in Syngas Production. *Sep. Purif. Technol.* **2020**, *236*, 116268.
(25) Tawalbeh, M.; Al-Ismaily, M.; Kruczek, B.; Tezel, F. H. Modeling the Transport of CO2, N2, and Their Binary Mixtures through Highly Permeable Silicalite-1 Membranes Using Maxwell−Stefan Equations. *Chemosphere* **2021**, *263*, 127935.
(26) Wilson, S. M. W.; Gabriel, V. A.; Tezel, F. H. Adsorption of Components from Air on Silica Aerogels. *Microporous Mesoporous Mater.* **2020**, *305*, 110297.
(27) Zhai, Y.; Chuang, S. S. C. Enhancing Degradation Resistance of Polyethylenimine for CO_2 Capture with Cross-Linked Poly(Vinyl Alcohol). *Ind. Eng. Chem. Res.* **2017**, *56*, 13766−13775.
(28) Yu, J.; Zhai, Y.; Chuang, S. S. C. Water Enhancement in CO_2 Capture by Amines: An Insight into CO_2-H_2O Interactions on Amine Films and Sorbents. *Ind. Eng. Chem. Res.* **2018**, *57*, 4052−4062.
(29) Miller, D. D.; Yu, J.; Chuang, S. S. C. Unraveling the Structure and Binding Energy of Adsorbed CO2/H2O on Amine Sorbents. *J. Phys. Chem. C* **2020**, *124*, 24677−24689.
(30) Yu, J.; Chuang, S. S. C. The Structure of Adsorbed Species on Immobilized Amines in CO_2 Capture: An in Situ IR Study. *Energy Fuels* **2016**, *30*, 7579−7587.
(31) Yu, J.; Chuang, S. S. C. The Role of Water in CO_2 Capture by Amine. *Ind. Eng. Chem. Res.* **2017**, *56*, 6337−6347.
(32) Sujan, A. R.; Kumar, D. R.; Sakwa-Novak, M.; Ping, E. W.; Hu, B.; Park, S. J.; Jones, C. W. Poly(Glycidyl Amine)-Loaded SBA-15 Sorbents for CO_2 Capture from Dilute and Ultradilute Gas Mixtures. *ACS Appl. Polym. Mater.* **2019**, *1*, 3137−3147.
(33) Park, S. J.; Lee, J. J.; Hoyt, C. B.; Kumar, D. R.; Jones, C. W. Silica Supported Poly(Propylene Guanidine) as a CO2 Sorbent in Simulated Flue Gas and Direct Air Capture. *Adsorption* **2020**, *26*, 89−101.
(34) Kumar, D. R.; Rosu, C.; Sujan, A. R.; Sakwa-Novak, M. A.; Ping, E. W.; Jones, C. W. Alkyl-Aryl Amine-Rich Molecules for CO2Removal via Direct Air Capture. *ACS Sustainable Chem. Eng.* **2020**, *8*, 10971−10982.
(35) Rosu, C.; Pang, S. H.; Sujan, A. R.; Sakwa-Novak, M. A.; Ping, E. W.; Jones, C. W. Effect of Extended Aging and Oxidation on Linear Poly(Propylenimine)-Mesoporous Silica Composites for CO2Capture from Simulated Air and Flue Gas Streams. *ACS Appl. Mater. Interfaces* **2020**, *12*, 38085−38097.
(36) Anyanwu, J. T.; Wang, Y.; Yang, R. T. Amine-Grafted Silica Gels for CO_2 Capture Including Direct Air Capture. *Ind. Eng. Chem. Res.* **2020**, *59*, 7072−7079.
(37) Harlick, P. J. E.; Sayari, A. Applications of Pore-Expanded Mesoporous Silicas. 3. Triamine Silane Grafting for Enhanced CO_2 Adsorption. *Ind. Eng. Chem. Res.* **2006**, *45*, 3248−3255.

https://doi.org/10.1021/acs.iecr.1c00415
Ind. Eng. Chem. Res. 2021, 60, 6277−6286

(38) Sujan, A. R.; Pang, S. H.; Zhu, G.; Jones, C. W.; Lively, R. P. Direct CO_2Capture from Air Using Poly(Ethylenimine)-Loaded Polymer/Silica Fiber Sorbents. *ACS Sustainable Chem. Eng.* **2019**, *7*, 5264−5273.
(39) Wang, Y.; Yang, R. T. Template Removal from SBA-15 by Ionic Liquid for Amine Grafting: Applications to CO_2 Capture and Natural Gas Desulfurization. *ACS Sustainable Chem. Eng.* **2020**, *8*, 8295−8304.
(40) Yuan, M. H.; Wang, L.; Yang, R. T. Glow Discharge Plasma-Assisted Template Removal of SBA-15 at Ambient Temperature for High Surface Area, High Silanol Density, and Enhanced CO_2 Adsorption Capacity. *Langmuir* **2014**, *30*, 8124−8130.
(41) Wang, L.; Yang, R. T. Increasing Selective CO_2 Adsorption on Amine-Grafted SBA-15 by Increasing Silanol Density. *J. Phys. Chem. C* **2011**, *115*, 21264−21272.
(42) Feng, X.; Fryxell, G. E.; Wang, L. Q.; Kim, A. Y.; Liu, J.; Kemner, K. M. Functionalized Monolayers on Ordered Mesoporous Supports. *Science* **1997**, *276*, 923−926.
(43) Harlick, P. J. E.; Sayari, A. Applications of Pore-Expanded Mesoporous Silica. 5. Triamine Grafted Material with Exceptional CO_2 Dynamic and Equilibrium Adsorption Performance. *Ind. Eng. Chem. Res.* **2007**, *46*, 446−458.
(44) Jahandar Lashaki, M.; Sayari, A. CO2 Capture Using Triamine-Grafted SBA-15: The Impact of the Support Pore Structure. *Chem. Eng. J.* **2018**, *334*, 1260−1269.
(45) Wang, L.; Yin, C.; Yang, R. T. Selective Catalytic Reduction of Nitric Oxide with Hydrogen on Supported Pd: Enhancement by Hydrogen Spillover. *Appl. Catal. A Gen.* **2016**, *514*, 35−42.
(46) Chen, S.-Y.; Chen, Y.-T.; Lee, J.-J.; Cheng, S. Tuning Pore Diameter of Platelet SBA-15 Materials with Short Mesochannels for Enzyme Adsorption. *J. Mater. Chem.* **2011**, *21*, 5693−5703.
(47) Kruk, M.; Jaroniec, M.; Sayari, A. Application of Large Pore MCM-41 Molecular Sieves to Improve Pore Size Analysis Using Nitrogen Adsorption Measurements. *Langmuir* **1997**, *13*, 6267−6273.
(48) Sing, K. S.; Everett, D. H.; Haul, R. A. W.; Moscou, L.; Pierotti, R. A.; Rouquerol, J.; Siemieniewska, T. Reporting physisorption data for gas/solid systems with special reference to the determination of surface area and porosity (Recommendations 1984). *Pure Appl. Chem.* **1985**, *57*, 603−619.
(49) Assink, R. A.; Kay, B. D. SOL-GEL KINETICS I. Functional Group Kinetics. *J. Non-Cryst. Solids* **1988**, *99*, 359−370.
(50) Arkles, B.; Steinmetz, J. R.; Zazyczny, J.; Mehta, P. Factors Contributing to the Stability of Alkoxysilanes in Aqueous Solution. *J. Adhes. Sci. Technol.* **1992**, *6*, 193−206.
(51) Sánchez-Zambrano, K.; Duarte, L. L.; Maia, D. S.; Vilarrasa-García, E.; Bastos-Neto, M.; Rodríguez-Castellón, E.; de Azevedo, D. C. S. CO_2 Capture with Mesoporous Silicas Modified with Amines by Double Functionalization: Assessment of Adsorption/Desorption Cycles. *Materials* **2018**, *11*, 887.
(52) Fan, Y.; Labreche, Y.; Lively, R. P.; Jones, C. W.; Koros, W. J. Dynamic CO_2 Adsorption Performance of Internally Cooled Silica-Supported Poly(Ethylenimine) Hollow Fiber Sorbents. *AIChE J.* **2014**, *60*, 3878−3887.
(53) Zhang, G.; Zhao, P.; Xu, Y. Development of Amine-Functionalized Hierarchically Porous Silica for CO2 Capture. *J. Ind. Eng. Chem.* **2017**, *54*, 59−68.
(54) Epiepang, F. E.; Li, J.; Liu, Y.; Yang, R. T. Low-Pressure Performance Evaluation of CO2, H2O and CH4 on Li-LSX as a Superior Adsorbent for Air Prepurification. *Chem. Eng. Sci.* **2016**, *147*, 100−108.
(55) Wang, Y.; Yang, R. T. Chemical Liquid Deposition Modified 4A Zeolite as a Size-Selective Adsorbent for Methane Upgrading, CO_2 Capture and Air Separation. *ACS Sustainable Chem. Eng.* **2019**, *7*, 3301−3308.
(56) Sayari, A.; Belmabkhout, Y. Stabilization of Amine-Containing CO_2 Adsorbents: Dramatic Effect of Water Vapor. *J. Am. Chem. Soc.* **2010**, *132*, 6312−6314.
(57) Stuckert, N. R.; Yang, R. T. CO2 Capture from the Atmosphere and Simultaneous Concentration Using Zeolites and Amine-Grafted SBA-15. *Environ. Sci. Technol.* **2011**, *45*, 10257−10264.
(58) Wang, L.; Yang, R. T. New Nanostructured Sorbents for Desulfurization of Natural Gas. *Front. Chem. Sci. Eng.* **2014**, *8*, 8−19.
(59) Sanz-Pérez, E. S.; Murdock, C. R.; Didas, S. A.; Jones, C. W. Direct Capture of CO_2 from Ambient Air. *Chem. Rev.* **2016**, *116*, 11840−11876.
(60) Loganathan, S.; Ghoshal, A. K. Amine Tethered Pore-Expanded MCM-41: A Promising Adsorbent for CO_2 capture. *Chem. Eng. J.* **2017**, *308*, 827−839.
(61) Kishor, R.; Ghoshal, A. K. APTES Grafted Ordered Mesoporous Silica KIT-6 for CO2 adsorption. *Chem. Eng. J.* **2015**, *262*, 882−890.
(62) Hiyoshi, N.; Yogo, K.; Yashima, T. Adsorption of Carbon Dioxide on Amine Modified SBA-15 in the Presence of Water Vapor. *Chem. Lett.* **2004**, *33*, 510−511.
(63) Mittal, N.; Samanta, A.; Sarkar, P.; Gupta, R. Postcombustion CO2 Capture Using N-(3-Trimethoxysilylpropyl)Diethylenetriamine-Grafted Solid Adsorbent. *Energy Sci. Eng.* **2015**, *3*, 207−220.

https://doi.org/10.1021/acs.iecr.1c00415
Ind. Eng. Chem. Res. 2021, 60, 6277−6286